



---

*Research article*

## **A survey of conformational and energetic changes in G protein signaling**

**Alyssa D. Lokits**<sup>1</sup>, **Julia Koehler Leman**<sup>2</sup>, **Kristina E. Kitko**<sup>1,3</sup>, **Nathan S. Alexander**<sup>4</sup>, **Heidi E. Hamm**<sup>1,5</sup>, and **Jens Meiler**<sup>1,5,6,\*</sup>

<sup>1</sup> Neuroscience Department, Vanderbilt University, TN, USA

<sup>2</sup> Chemical and Biomolecular Engineering Department, Johns Hopkins University, MD, USA

<sup>3</sup> Engineering Department, Vanderbilt University, TN, USA

<sup>4</sup> Pharmacology Department, Case Western Reserve University, OH, USA

<sup>5</sup> Pharmacology Department, Vanderbilt University, TN, USA

<sup>6</sup> Chemistry Department, Vanderbilt University, TN 3722-6600, USA

\* **Correspondence:** Email: [info@meilerlab.org](mailto:info@meilerlab.org); Tel: 615-936-5662;  
Fax: 615-936-221.

**Abstract:** Cell signaling is a fundamental process for all living organisms. G protein-coupled receptors (GPCRs) are a large and diverse group of transmembrane receptors which convert extracellular signals into intracellular responses primarily via coupling to heterotrimeric G proteins. In order to integrate the range of very diverse extracellular signals into a message the cell can recognize and respond to, conformational changes occur that rewire the interactions between the receptor and heterotrimer in a specific and coordinated manner. By interrogating the energetics of these interactions within the individual proteins and across protein-protein interfaces, a communication network between amino acids involved in conformational changes for signaling, is created. To construct this mapping of pairwise interactions *in silico*, we analyzed the Rhodopsin GPCR coupled to a G $\alpha$ 1 $\beta$ 1 $\gamma$ 1 heterotrimer. The structure of this G protein complex was modeled in the receptor-bound and unbound heterotrimeric states as well as the activated, monomeric G $\alpha$ (GTP) state. From these tertiary structural models, we computed the average pairwise residue-residue interactions and interface energies across ten models of each state using the ROSETTA modeling software suite. Here we disseminate a comprehensive survey of all critical interactions and create intra-protein network communication maps. These networks represent nodes of interaction necessary for G protein activation.

**Keywords:** heterotrimeric G protein; G protein coupled receptor; energetic; ROSETTA; modeling; pairwise interactions

## Abbreviations

GDP	Guanosine diphosphate
GPCR	G Protein Coupled Receptor
GTP	Guanosine triphosphate
GTP $\gamma$ S	Guanosine 5'-[ $\gamma$ -thio]triphosphate
P-loop	phosphate binding loop
REU	ROSETTA Energy Units
r.m.s.d	root mean square deviation
$\Delta\Delta G$	delta, delta G binding interface energy

## 1. Introduction

G protein-coupled receptors (GPCRs) are the largest and most diverse class of membrane receptors in eukaryotes [1]; they bind many different types of ligands to initiate an array of intracellular signaling cascades. GPCRs primarily interact with membrane associated, heterotrimeric complexes called G proteins in order to transduce their extracellular signal into a cellular response. The three subunits,  $G\alpha$ ,  $\beta$ , and  $\gamma$ , undergo conformational changes to interact with different protein binding partners along their signaling cycle in order to transmit the appropriate messages within the cell [1,2].

The most dynamic changes in structure and affinity can be seen in the  $G\alpha$  subunit, which mitigates each step of the complex's signaling dynamics and function [3,4,5]. The affinity of the  $G\alpha$  subunit to each of its different binding partners is determined by the structural changes it undergoes within the signaling cycle [6]. Therefore one can think of the  $G\alpha$  subunit as the control center of this signal transducing machinery as it preferentially interacts with different proteins, complexes, and small molecules via conformational changes of its own structure to propagate the information to other signaling moieties within the cell (Figure 1A).

### 1.1. G protein signaling cycle

In its inactive state, the  $G\alpha$  subunit has a high affinity for the nucleotide GDP, possesses a closed helical domain, and interacts with the  $G\beta\gamma$  subunits. Upon interaction with an activated GPCR, the  $G\alpha$  subunit undergoes conformational changes to accommodate binding the receptor (Figure 1B) [5,7,8]. This includes the rigid body rotation of its  $\alpha 5$  helix up and into the receptor (Figure 2), as it moves along the hydrophobic  $\beta$ -sheets surrounding it to create new interactions sites within the GTPase domain and to the helical domain [9]. This rotation signals to the rest of the complex through an altered interaction network that the  $G\alpha$  subunit is bound to the receptor. In this receptor-bound conformation, the  $G\alpha$  subunit's affinity for GDP is drastically reduced as its flexible

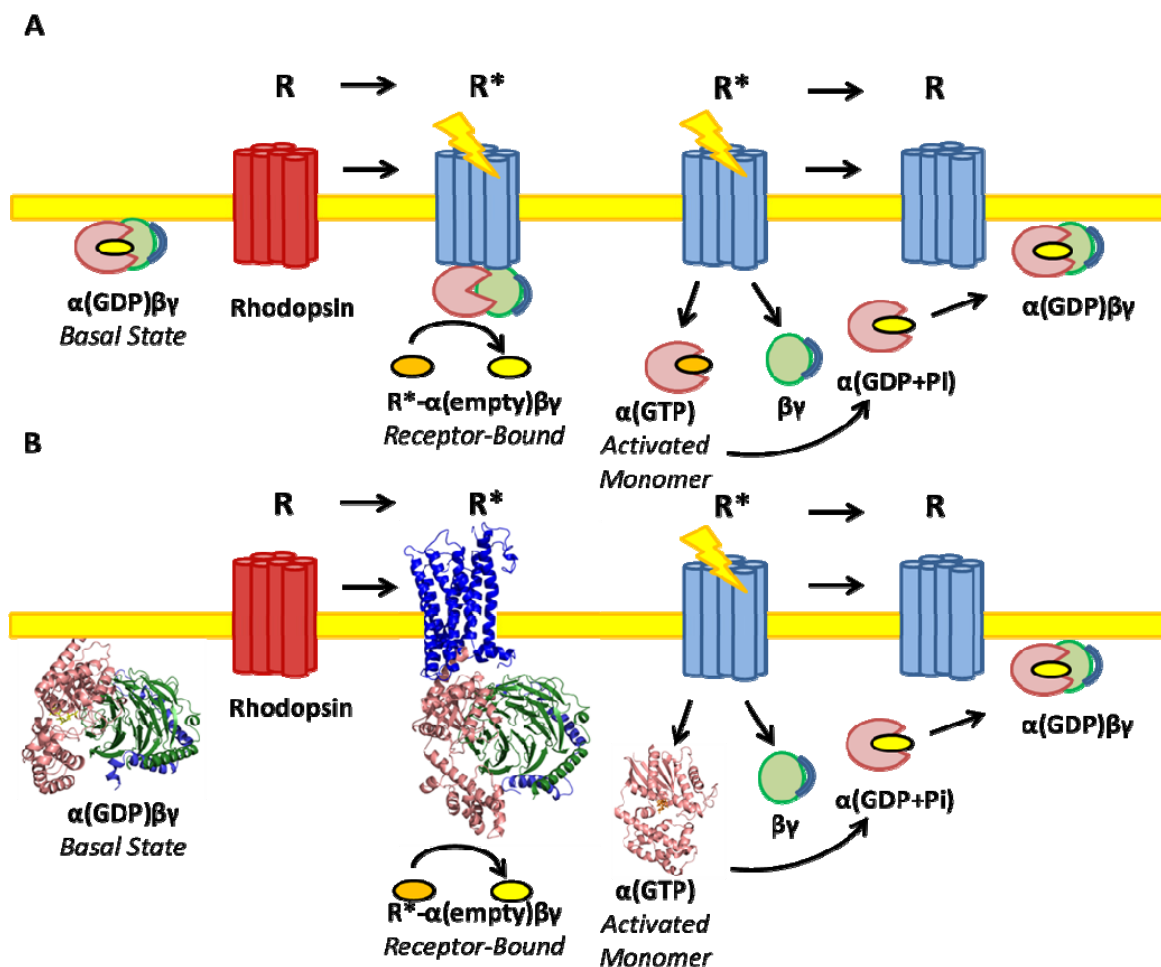


**Figure 1. G protein coupled receptors (GPCRs) typically signal through interaction with membrane-associated heterotrimeric G proteins. These proteins become activated via the exchange of GDP for GTP, induced by the activated receptor ( $\text{R}^*$ ). Upon this nucleotide exchange, the heterotrimer dissociates into the monomer  $\text{G}\alpha(\text{GTP})$  and  $\text{G}\beta\gamma$  dimer which may then interact with downstream signal effector proteins (not shown for clarity) to propagate and amplify intracellular signaling. The cycle is complete when  $\text{G}\alpha$  hydrolyzes GTP to GDP + Pi which allows the trimer to reassemble into the basal, non-signaling state. A) Linear schematic of the G protein signaling cycle. B) ROSETTA-derived structural representations of the three  $\text{G}\alpha$  states examined herein;  $\text{G}\alpha_{i1}(\text{GDP})\beta_1\gamma_1$ ,  $\text{R}^*\text{-G}\alpha_{i1}(\text{empty})\beta_1\gamma_1$ , and  $\text{G}\alpha_{i1}(\text{GTP})$ .**

helical domain opens to allow nucleotide escape [10]. Upon GDP release, the  $\text{G}\alpha$  subunit has a high affinity for GTP, though the nucleotides only differ in the addition of a single phosphate group. Once GTP is present in the binding pocket, the  $\text{G}\alpha$  subunit once again alters its conformation and affinity for both the activated receptor and the  $\text{G}\beta\gamma$  subunits bound to it. Subsequent dissociation of the  $\text{G}\alpha$  subunit from this complex frees  $\text{G}\alpha$ , as well as  $\text{G}\beta\gamma$ , to interact with downstream signaling effector proteins and regulator molecules in order to continue the signaling cascade [11]. In this GTP-bound, active conformation, the  $\text{G}\alpha$  subunit possesses different binding interfaces to interact with various

effector moieties [3,12]. The intrinsic enzymatic ability of  $G\alpha$  hydrolyzes GTP back to GDP [2]. The rate of hydrolysis can be altered by interacting with accessory proteins which alter the enzyme's catalytic efficiency [13]. Upon cleavage of the  $\gamma$  phosphate group, the  $G\alpha$  subunit structure returns to its basal state where its propensity to complex with  $G\beta\gamma$  is once again higher than its affinity to interact with other signaling moieties; the reunion of the heterotrimer allows the signaling cycle to terminate or for the complex to begin additional rounds of signaling [1].

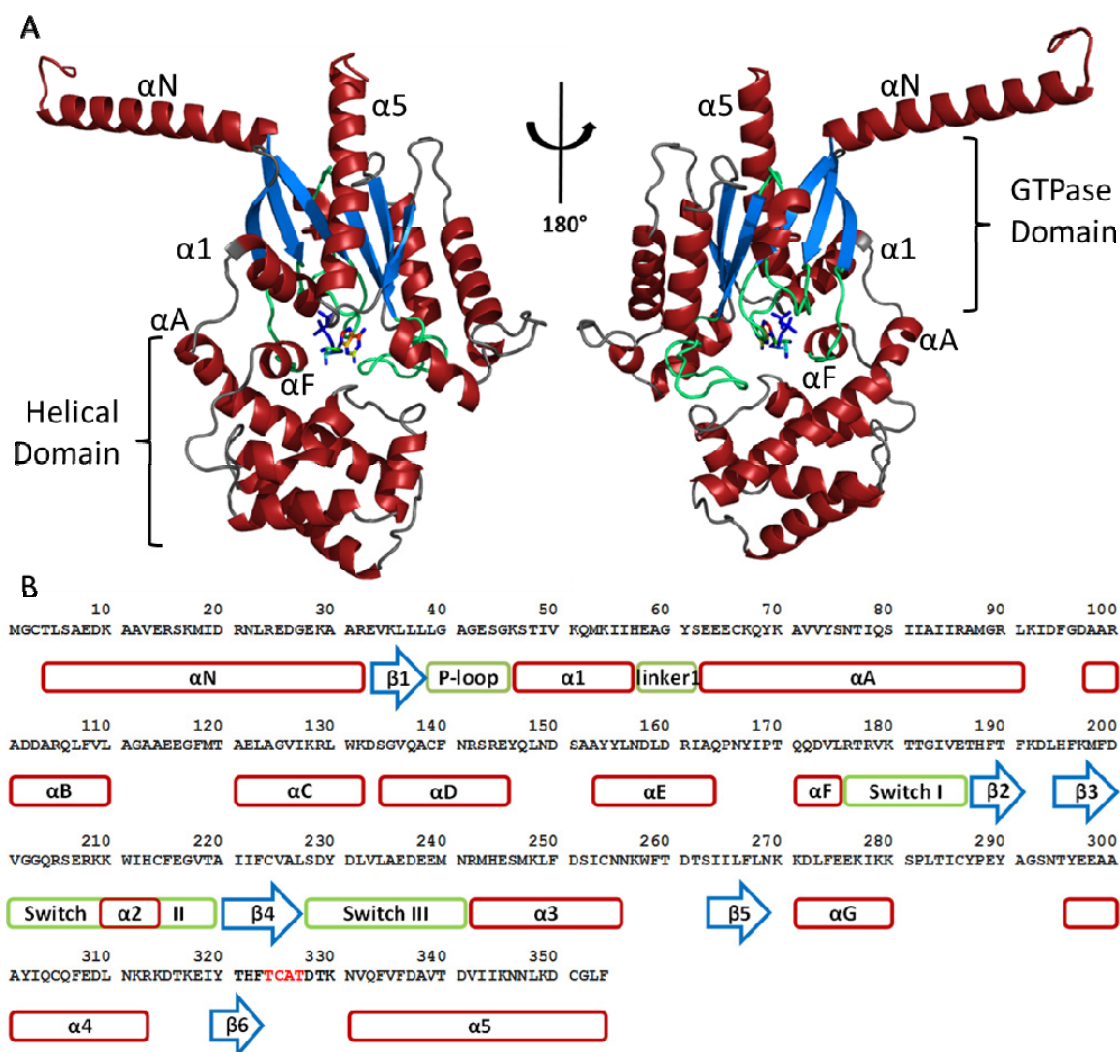


**Figure 2.** A) Representative  $G\alpha_{i1}$ (GDP) structure in the basal state ( $\beta_1\gamma_1$  removed for clarity) and rotated  $180^\circ$ . Basal nucleotide (GDP) is depicted in dark blue. B) The sequence is derived from rat  $G\alpha_{i1}$ . Secondary structure elements (red—helices, blue—sheets, and green—critical loop regions) are labeled as described in [3].

## 1.2. Significance

Current progress in crystallization of GPCRs has greatly aided in our understanding of the G protein's role within the ternary complex model. Recent work from the Kobilka laboratory has provided the first glimpse of an activated GPCR, the  $\beta_2$ -Adrenergic receptor, in complex with a  $G\alpha_s$  heterotrimeric G protein [5]. However, the experimental structure does not provide information on

the energetic interactions between amino acids critical for the signaling process. What are the energetic contributions of interactions, broken and newly made, that move the signal from the receptor to the nucleotide binding site? Such an analysis is complicated as the experimental structure presents a static image of interactions in a dynamic system. Crystal structures alone cannot show the conformational dynamics the  $G\alpha$  subunit must continue to undergo to propagate information to the rest of the complex. Further, the use of nanobodies, mutations, and various crystallization aids can alter physiologically relevant conformations of the protein to achieve the most energetically stable interactions for crystal formation.

To better understand the modulatory process the  $G\alpha$  subunit undergoes to propagate its signaling information, an energetic analysis of these conformational changes was performed. We introduce a new pairwise, residue-residue assessment of protein side chain and backbone interactions to describe tertiary topology. Using the available crystallographic structures of each conformation the  $G\alpha$  subunit progresses through during different signaling states, we have created interaction network “maps”. Specifically, we have chosen to investigate the heterotrimeric G protein  $\alpha$  subunit in its basal, receptor-unbound  $G\alpha_{i1}(\text{GDP})\beta\gamma$  state, the receptor-bound  $R^*-G\alpha_{i1}(\text{empty})\beta\gamma$  state, and the activated, monomeric  $G\alpha_{i1}(\text{GTP})$  state using the protein software suite, ROSETTA (Figure 1B).

Understanding the mechanism of cellular signaling is a crucial step in understanding the biology of any living organism. This article analyzes changes in conformational and structural information by evaluating the predicted energy of interactions required to maintain function of the  $G\alpha$  subunit before, during, and after binding with the membrane-bound receptor. The ROSETTA protein modeling software allows interrogation of intra-protein and inter-protein interactions on the amino acid level. Using an established comparative modeling protocol [14,15] and binding interface analysis [16,17], we have created the first comprehensive framework for interrogation of pairwise amino acid interactions across each of the signaling states. This analysis has allowed us to create predictive communication maps between interacting side chain pairs throughout the  $G\alpha$  structure as the conformational shifts propagate.

## 2. Materials and Methods

### 2.1. Models

To create interaction networks within the different signaling states of the G protein  $\alpha$  subunit, we have combined several methodologies. Using previously published comparative models of the GPCR- $G\alpha_{i1}$  heterotrimeric proteins [9], we have created an ensemble of structures for both the basal  $G\alpha_{i1}(\text{GDP})\beta\gamma$  and the receptor-bound  $R^*-G\alpha_{i1}(\text{empty})\beta\gamma$  states. Likewise, we have utilized the available crystal structures of activated, monomeric  $G\alpha_{i1}$  for a similar analysis (PDBIDs: 1GIA, 1GIL). Each structure of activated  $G\alpha_{i1}$  was energy-minimized in the presence of its GTP-analogue. To ensure a robust sampling of the backbone and side chain conformational space consistent with low energy, 500 models were created based on a  $G\alpha_i$  crystal structure (PDBID 1GIA). As more extensive sampling with 1000 poses was not shown to greatly increase model quality, generation of 500 models was used for all other structures. This is consistent with the findings of previous protocols [9]. Of these models, the ten lowest scoring models by ROSETTA score were shown to cover the spread of structural flexibility without allowing for larger structural deviations (Supplemental Figure 1). These ten models were employed for further analysis. For all analyses

herein, each model possessed the appropriate nucleotide for the given signaling state during all calculations.

## 2.2. $\Delta\Delta G$

From these initial models we then probed for intra- and intermolecular interaction energies using the ROSETTA computer modeling software suite. Three signaling states of the G protein  $\alpha$  subunit were addressed:  $G\alpha_{i1}(\text{GDP})\beta\gamma$ ,  $R^*-G\alpha_{i1}(\text{empty})\beta\gamma$ , and  $G\alpha_{i1}(\text{GTP})$  (Figure 1B). For each state, the binding interface energy ( $\Delta\Delta G$ ) was calculated for various key inter-protein interfaces across the complex and within the GTPase and the helical domains of the  $G\alpha$  subunit. Regions for analysis were selected for their roles as protein-protein interfaces or for their apparent role in maintaining protein stability within each conformational state. Specifically, key secondary structure elements (Figure 2) were evaluated for their ability to contribute to overall protein stability by calculating the changes in free energy before and after removal from the structure. Note that all energies are given in ROSETTA Energy Units (REUs) and include predicted contributions of van der Waals interactions, desolvation effects, hydrogen bonds, and electrostatics. While the ROSETTA-predicted energy has been shown to correlate with the free energy in kcal/mol [16,17], it is important to highlight that inaccuracies in the structural models and simplifications in the ROSETTA energy function lead to deviations between predicted and experimentally observed energies. Furthermore, the internal energy of small molecules is assumed to be unaltered upon binding to the protein; the energy measurements herein reflect energy perturbations induced by the ligand when binding to the protein. All  $\Delta\Delta G$  results are reported as the absolute value of REU scores for consistency with previously published data [9].

## 2.3. *Pairwise interaction score analysis*

Each of the three signaling states of the  $G\alpha_{i1}$  subunit were then interrogated at the amino acid level utilizing ROSETTA's pairwise score breakdown assessment. This feature calculates the interaction score for each possible amino acid pair. Note, that while this score is also measured in ROSETTA Energy Units (REUs) it is *not* a free energy in the thermodynamic sense. We therefore call these values consistently 'interaction scores'. However, this analysis allows for intra-molecular probing of information flow across signaling states while creating a network of stabilizing amino acid interactions. A protocol capture for this application has been validated externally and is available for public use within the ROSETTA framework. Herein, we apply this method to the G protein  $\alpha_{i1}$  subunit to highlight the method's effectiveness in predicting relevant structural nuances. Each of the signaling states of  $G\alpha_{i1}$  were assessed by averaging the per-residue contribution of the top ten lowest scoring models. The appropriate nucleotides and subunits were present throughout all calculations.

## 2.4. *Pairwise interaction score calculation*

Pairwise interaction scores were calculated using the ROSETTA software suite. The per residue score breakdown was calculated on ten comparative models which were created as previously described [9].

```
/residue_energy_breakdown.linuxgccrelease -database /rosetta/main/database/ -in:files:s <list
individual pdbs> -output:prefix <output file name> -restore_pre_talaris_2013_behavior
```

## 2.5. Protocols for pairwise interaction score analysis

Average per residue interaction pairs were calculated across ten models per signaling state in MATLAB using the following script:

```
file_1 = 'model_1.xlsm';
[~,~, raw_1] = xlsread(file_1);
model_1 = zeros(5223,3);
model_1(:,1) = cell2mat(raw_1(1:end,3));
model_1(:,2) = cell2mat(raw_1(1:end,5));
model_1(:,3) = cell2mat(raw_1(1:end,26));
new_matrix_1 = nan(354,354);
for i = 1:size(model_1)
    new_matrix_1(model_1(i,1),model_1(i,2))= model_1(i,3);
end
```

Continued for all models analyzed, then average scores across all models:

```
ave_matrix = nan(354,354);
for ii = 1:354
    for jj = 1:354
        ave_matrix(ii,jj) = mean([new_matrix_1(ii,jj) new_matrix_2(ii,jj) new_matrix_3(ii,jj) etc.]);
    end
end
g = ave_matrix(~isnan(ave_matrix));
[i,j] = ind2sub(size(ave_matrix), find(~isnan(ave_matrix)));
fin = [i,j,g];
```

## 2.6. Protocol capture

For further breakdown of all computational methods utilized herein, please refer to the companion Protocol Capture. All *in silico* methods and calculations were graciously verified by an external reviewer, Dr. J. Koehler Leman, Chemical and Biomolecular Engineering, Johns Hopkins University, Baltimore, MD.



### 3. Results

#### 3.1. Estimating free energy changes across protein-protein interfaces

Predicting free energy changes across protein-protein interfaces has been a staple in understanding the dynamics and kinetics of protein-protein interaction [16,18,19]. Used as a measure of binding efficiency,  $\Delta\Delta G$  estimates are a useful means of probing the thermodynamic stability of a protein interface in the bound and unbound states [9,19,20]. For our purposes, we utilized this measure to assess the energetic contribution secondary structure elements possessed along intra-protein interfaces between the helical and GTPase domains as well as for inter-domain stability.

For our calculations, specific secondary structure elements (Figure 2) were evaluated for their ability to contribute to overall protein stability by calculating the changes in free energy before and after their removal from the subunit structure. For all calculations, the appropriate nucleotides were present. The top ten lowest scoring models for the  $G\alpha_{i1}(\text{GDP})\beta\gamma$ ,  $R^*-G\alpha_{i1}(\text{empty})\beta\gamma$ , and  $G\alpha_{i1}(\text{GTP})$  states were each assessed, and their ROSETTA scores were averaged.

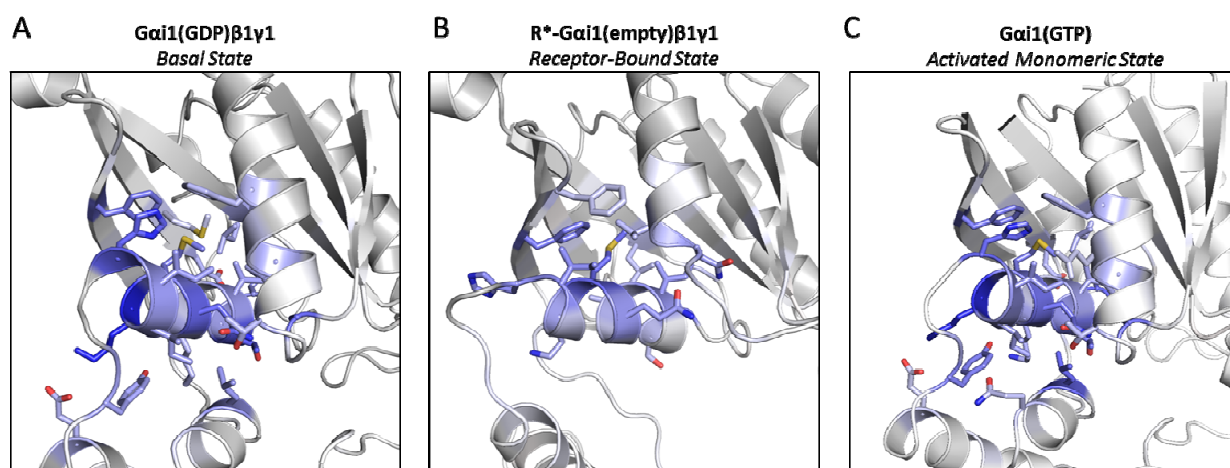


**Figure 3. Structural representation of predicted  $\Delta\Delta G$  of the  $\alpha 1$  helix across three states of  $G\alpha$  signaling— $G\alpha_{i1}(\text{GDP})\beta_1\gamma_1$ ,  $R^*-G\alpha_{i1}(\text{empty})\beta_1\gamma_1$ , and  $G\alpha_{i1}(\text{GTP})$ . The  $\alpha 1$  helix was defined as residues G45-E58 based on rat *Gai1* sequence. All calculations were averaged across the top ten scoring models for each state. Values reported here represent the absolute values of Rosetta Energy Units (REUs). REUs above 0.5 are considered significant. Residue contributions to the interface are color coded to indicate a greater contribution to stability. Lighter blue indicate a lower REU value relative to the darker shades.**

##### 3.1.1. GDP vs. GTP-bound models

The  $G\alpha$  subunit possesses similar energy in both the basal,  $G\alpha_{i1}(\text{GDP})\beta\gamma$ , and activated,  $G\alpha_{i1}(\text{GTP})$ , states. This is expected as the two states differ only in the addition of a  $\gamma$ -phosphate ion. Though the  $G\beta\gamma$  subunits were present for the basal calculations of the trimer, they do not



significantly alter  $G\alpha$ 's energetics when evaluating regions such as the  $\alpha 1$ ,  $\alpha 5$ , or  $\alpha F$  helices (Figures 3–4, and Supplemental Tables 1–3). When evaluating these regions, the resulting energies highlight a consistency between these two states suggesting that any structural changes within these regions begin and end with similar energies of interaction.

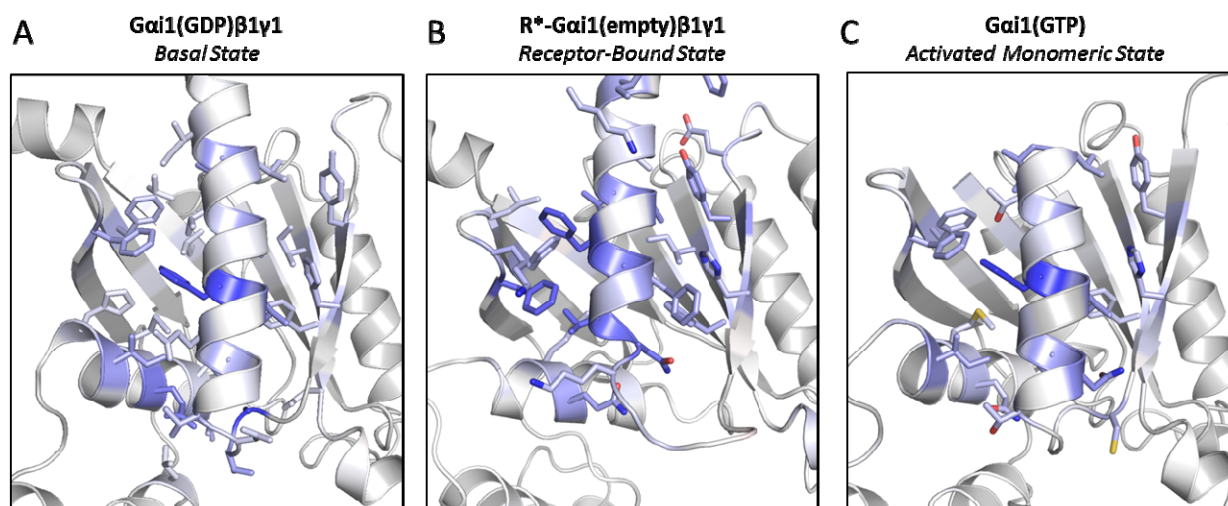


**Figure 4. Structural representation of predicted  $\Delta\Delta G$  of the  $\alpha 5$  helix across three states of  $G\alpha$  signaling— $G\alpha_{i1}(\text{GDP})\beta_1\gamma_1$ ,  $R^*\text{-}G\alpha_{i1}(\text{empty})\beta_1\gamma_1$ , and  $G\alpha_{i1}(\text{GTP})$ . The  $\alpha 5$  helix was extended to include part of the TCAT motif and is defined as residues C325-F354 based on rat *Gai1* sequence. All calculations were averaged across the top ten scoring models for each state. Values reported here represent the absolute values of ROSETTA Energy Units (REUs). REUs above 0.5 are considered significant. Residue contributions to the interface are color coded to indicate a greater contribution to stability. Lighter blue indicate a lower REU value relative to the darker shades. \*Note:  $G\alpha_{i1}(\text{GTP})$  crystal structure only extends to residue I343 preventing analysis of the  $\alpha 5$  helix beyond this residue in the activated, monomeric state.**

Noteworthy alterations in energies are seen around the nucleotide binding pocket and residues involved in stabilizing the  $G\beta$  interface between the basal and activated states. Examination of the P-loop and the variable Switch regions (I–III) (Figure 2) indicate more subtle  $\Delta\Delta G$  changes across these regions (Supplemental Tables 4–7). In the basal, trimeric state, the  $G\beta$  subunit organizes the loop regions into a binding interface. In its absence, the activated monomeric models do not show significant changes as seen in ROSETTA energy scores overall, though specific amino acid positions are reported to modulate.

### 3.1.2. Receptor-induced conformational changes

In contrast to the basal and activated states, the  $R^*\text{-}G\alpha_{i1}(\text{empty})\beta\gamma$  models show a stark transition in the communication network across the secondary structure elements of the  $G\alpha$  subunit. During this phase of the signaling cycle, the  $G\alpha$  subunit undergoes a large conformational change

which can be seen in the shifting of energetics around the  $\alpha 1$  helix, the  $\alpha 5$  helix (Figures 3–4, Supplemental Tables 1–2), and regions involved with nucleotide stability, namely the P-loop and the variable Switch (I–III) regions (Supplemental Table 4–7). It is during this stage of the signaling cycle that the receptor induces activation, the helical domain is opened, and the guanine nucleotide is allowed to exchange. The results from our models are consistent with experimental studies of these structural changes [9,10,21].

### 3.2. Predicting pairwise residue-residue contributions to protein stability

To interrogate the conformational changes that must occur at the amino acid network level between the signaling states, we devised a new application for the Rosetta modeling software's per-residue assessment of predicted interactions (publically available); this application allowed us to evaluate individual amino acid contributions to stability and function. For each of the three signaling states, the top ten models were assessed for each amino acid pair contribution to stability. The average score across the ten models was then plotted for each state (Figures 5–7, Supplemental Figures 2–8).

To evaluate which interactions were made and broken between the different signaling states, we compared the basal, heterotrimeric  $G\alpha_{i1}(GDP)\beta_1\gamma_1$  model scores to the receptor-bound,  $R^*G\alpha_{i1}(\text{empty})\beta_1\gamma_1$  and to the monomeric,  $G\alpha_{i1}(GTP)$  active state (Figure 5). From this calculation we show the variability of the Switch regions, as interactions are lost, or are diminished during receptor binding (red, above the diagonal) and remade in the active state (blue, below the diagonal). Some of this variability may be due to the loss of  $\beta_1\gamma_1$  binding upon activation.

The predicted opened and closed conformations of the helical domain are also recognized when evaluating residue-residue interactions across states. The receptor binding induces structural rearrangements that ultimately lead to helical domain opening [5,9,10,21]; therefore, the upper matrix, above the diagonal, indicates the helical domain must break contacts for activation (red). The basal and active  $G\alpha_{i1}$  subunits possess very similar secondary structure and tertiary fold. Therefore, fewer interactions are lost or diminished between the two states (below the diagonal). New interactions or more favorable interactions (blue) must be made to accommodate the GTP nucleotide and the lack of  $\beta_1\gamma_1$  subunits.

However, this broad representation does not do justice to the nuanced alterations of residue-residue interaction. In addition the overall number of intraprotein  $G\alpha$  interactions is not expected to change across the different signaling states as all secondary structure elements and the global tertiary fold is maintained. Though there are technically fewer intraprotein contacts when the helical domain is opened during the receptor bound state, these differences are subtracted from interaction scores that are present in the GDP-bound trimer; the result is a change in magnitude from interaction to no interaction that is recorded in this matrix. Additionally changes in magnitude for the pairwise interactions in the range of  $-0.5$  to  $0.5$  REU were removed to highlight more significant contributions.

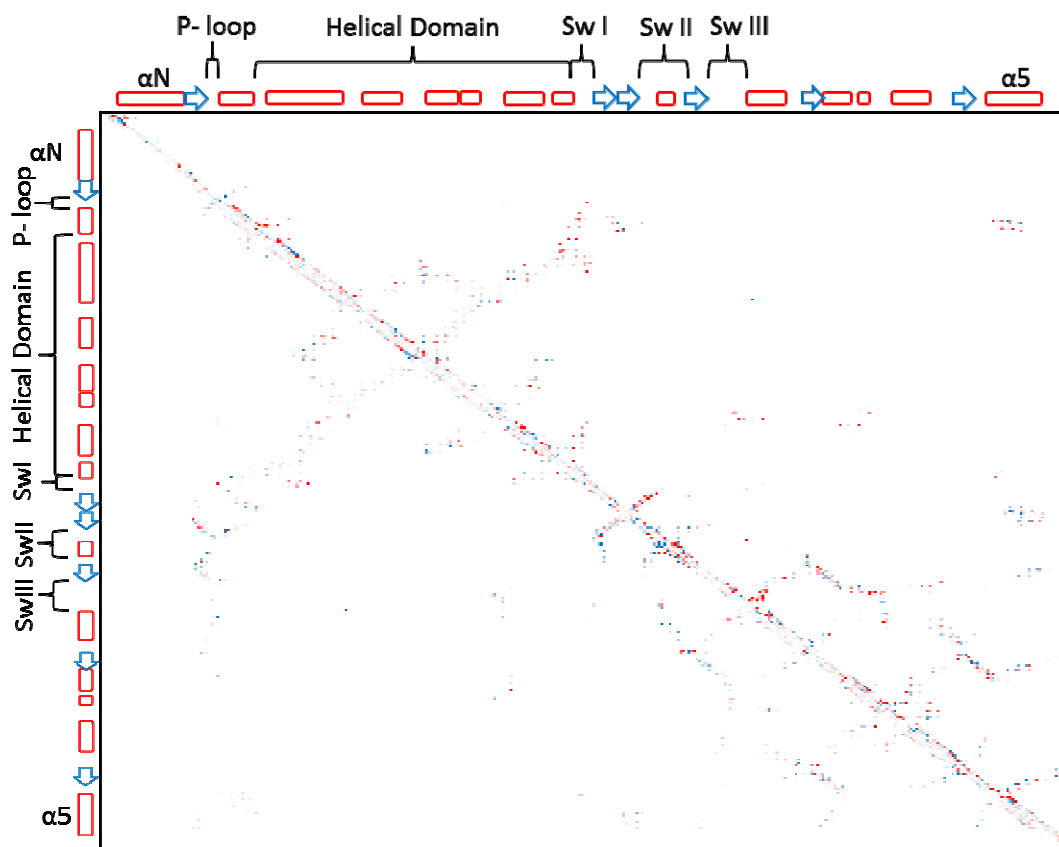


Figure 5. Pairwise analysis of ROSETTA scores for individual amino acid interactions as a means to monitor information networks across signaling states. These interaction networks represent side chain and backbone atom contributions to the stability and functionality of the protein structure. These matrices compare across the protein signaling states to investigate predicted interaction (and therefore structural) changes between residue pairs. The x- and y-axes represent each residue position of the  $G\alpha$  subunit compared across all other possible residue positions. Above the diagonal depicts the score difference (in REU) between the basal, heterotrimeric  $G\alpha_{i1}(GDP)\beta_1\gamma_1$  structure and the receptor-bound complex,  $R^*G\alpha_{i1}(empty)\beta_1\gamma_1$ . The lower matrix below the diagonal depicts the score difference (in REU) between the basal, heterotrimeric  $G\alpha_{i1}(GDP)\beta_1\gamma_1$  structure and the activated  $G\alpha_{i1}(GTP)$  monomeric subunit after dissociation from Rhodopsin and  $\beta_1\gamma_1$ . Only the  $G\alpha$  subunit's amino acid contributions are shown for clarity. Residue-residue interactions in the range of  $-0.5$  to  $0.5$  REU were removed to highlight more significant differences in contributions. Stabilizing residue interactions are depicted in red while a predicted loss of interaction scores are shown in blue. Note\* The crystal structures used for the monomeric  $G\alpha_{i1}(GTP)$  models lack residues 1–34, and 343–354. These residues are therefore removed from the analysis.

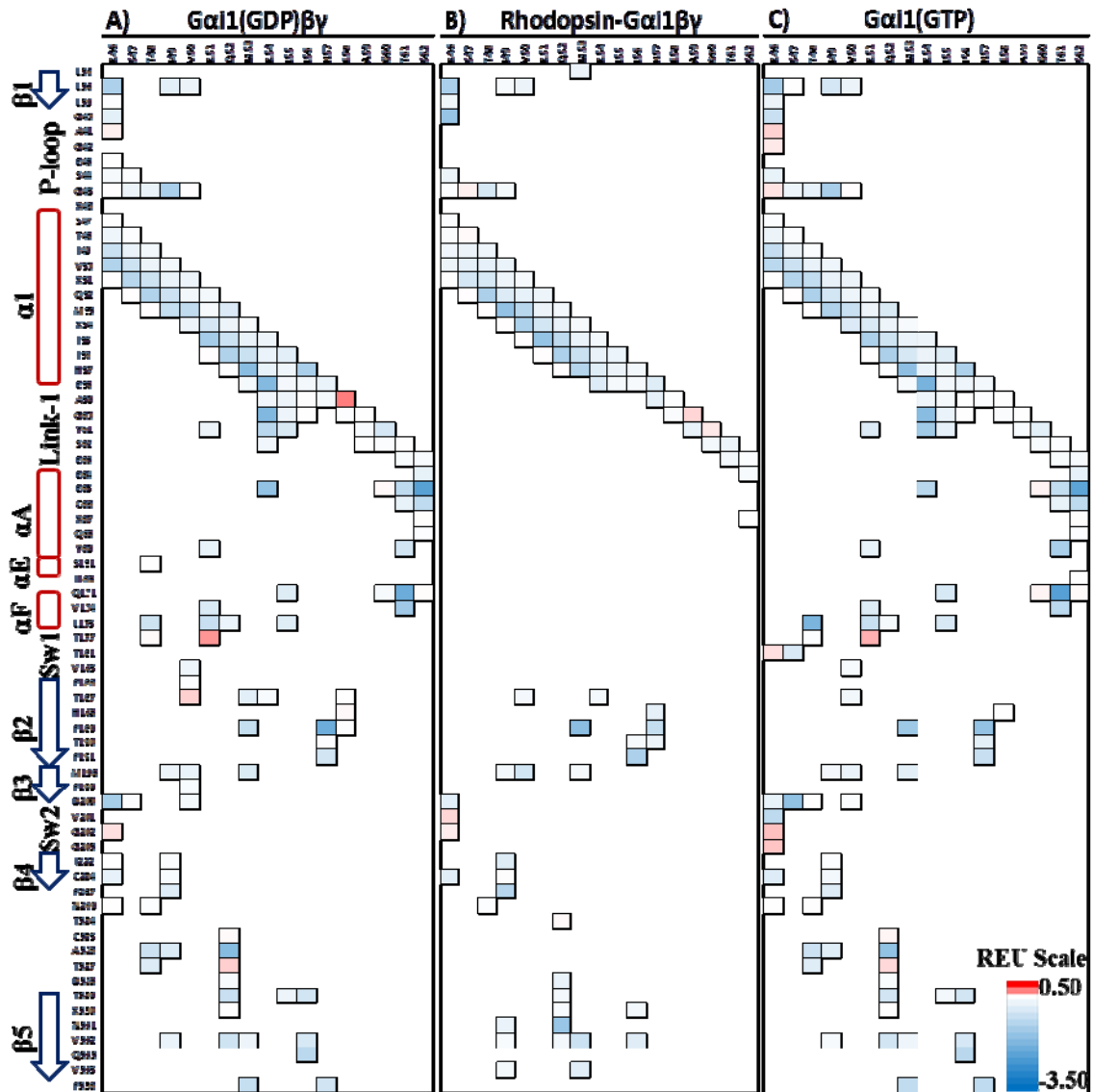
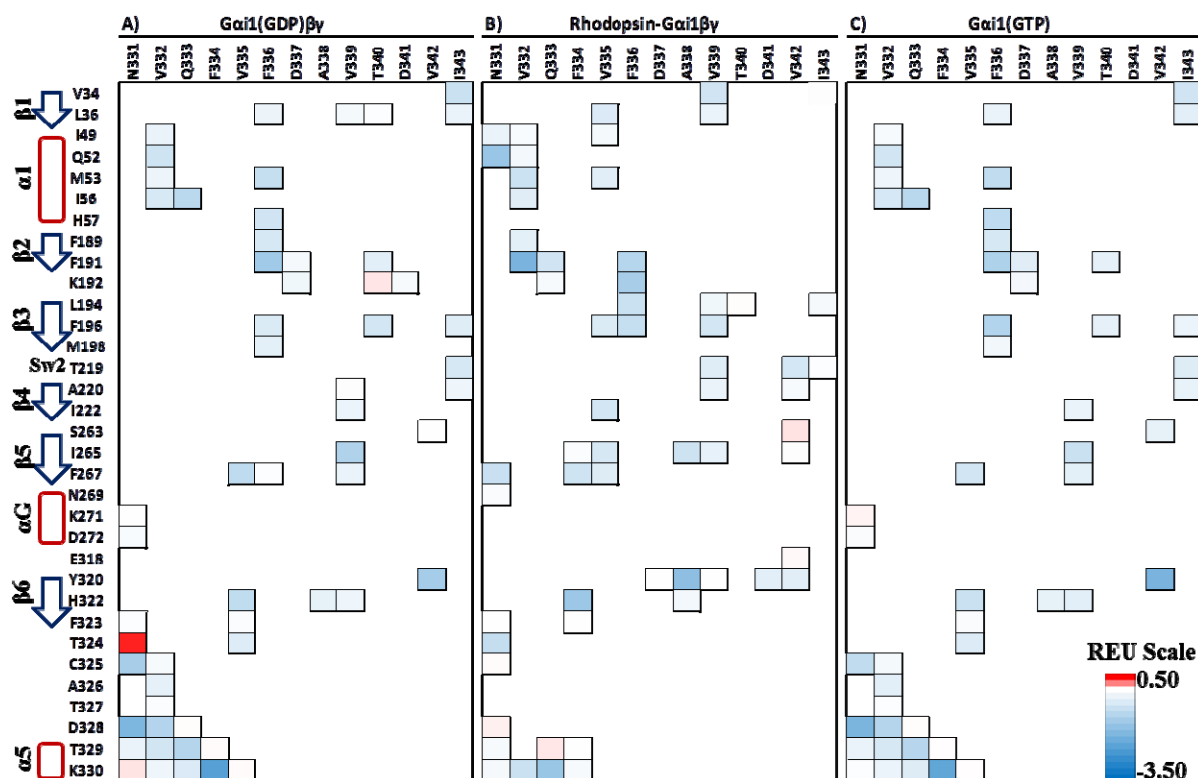


Figure 6. Pairwise analysis of individual amino acid interactions across three  $G\alpha$  signaling states to investigate changes between residue pairs interacting with the  $\alpha 1$  helix and Linker 1 region (K46-I56, & H57-S62, respectively). A) The heterotrimeric  $G\alpha_{i1}(GDP)\beta_1\gamma_1$  structure in the basal state. B) The heterotrimeric  $G\alpha_{i1}(\text{empty})\beta_1\gamma_1$  subunits interacting with the GPCR, Rhodopsin. C) The activated  $G\alpha_{i1}(GTP)$  monomeric subunit after dissociation from Rhodopsin and  $\beta_1\gamma_1$ . Only the  $G\alpha$  subunit's pairwise amino acid contributions are shown for A–C. REUs for individual pairs are color coded ranging from more stable predicted interaction scores (minimum  $-2.32$ ) in blue to positive, repulsive scores terms (maximum  $0.26$ ) in red.



**Figure 7. Pairwise analysis of individual amino acid interactions across three  $G\alpha$  signaling states to investigate changes between residue pairs interacting with the  $\alpha 5$  helix (N331-I343). A) The heterotrimeric  $G\alpha_{i1}(GDP)\beta_1\gamma_1$  structure in the basal state. B) The heterotrimeric  $G\alpha_{i1}(\text{empty})\beta_1\gamma_1$  subunits interacting with the GPCR, Rhodopsin. C) The activated  $G\alpha_{i1}(GTP)$  monomeric subunit after dissociation from Rhodopsin and  $\beta_1\gamma_1$ . Only the  $G\alpha$  subunit's amino acid contributions are shown for A–C. REUs for individual pairs are color coded ranging from more stable predicted interaction scores (minimum  $-2.30$ ) in blue to positive, repulsive score terms (maximum  $0.31$ ) in red. \*Note:  $G\alpha_{i1}(GTP)$  crystal structure lacks residues 344–354 preventing analysis of the full carboxyl terminus.**

### 3.2.1. The Switch Regions

Across the three signaling states, a pattern of interaction emerges. As seen with the  $\Delta\Delta G$  calculations (Figures 3–4, Supplemental Tables 1–8), the basal and activated  $G\alpha$  subunits maintain similar amino acid interactions. However, the  $\gamma$  phosphate group present in the activated  $G\alpha$  monomer leads to shifts in the communication networks of the Switch I-III regions (Supplemental Figures 2–4). As implied by their name, these regions have been shown to alter their conformation in the presence of GTP instead of GDP in crystal structures [22,23].

The largest shift among these three elements is shown in the Switch II region (Supplemental Figure 3). This is expected as the Switch II region also interfaces with the  $G\beta$  subunit. Present in this analysis during the trimeric basal and receptor-bound states, the pairwise interaction map of  $G\beta$  with the Switch II region maintains interaction similarity and therefore structural similarity between these

two states. Key differences can be seen around the Switch I and  $\beta 2$  elements with which the Switch II region interacts in the GDP-bound state, but not during the receptor bound state.

Alterations in the communication network along the  $G\beta$  subunit itself were not the primary focus of the current study; however, the  $G\beta/G\gamma$  subunits were present for the analysis of the basal and receptor-bound states. Therefore, they are included as interaction partners along the corresponding interface residues. Interestingly, the  $G\beta$  subunit does show an altered conformation network between the receptor-unbound and bound states suggesting some flexibility between the two G protein subunits. This modulation of the  $G\alpha$  Switch II region does not seem to show similar intra-protein interaction flexibility within the  $G\alpha$  subunit itself, but rather it highlights relevant changes within the heterotrimeric complex which may contribute to the mechanisms of receptor induced activation.

### 3.2.2. Rearrangements from nucleotide exchange

With this detailed analysis, we show that more elements other than the Switch regions possess an altered communication network. Subtle changes in the  $\alpha 1$  helix,  $\alpha 5$  helix,  $\alpha F$  helix and P-loop highlight structural alterations induced by the nucleotide (Figures 6–7, Supplemental Figures 5–6). Specifically, the GDP-bound versus GTP-bound  $G\alpha$  subunit show altered network intensities along the  $\beta 6$ - $\alpha 5$  loop within the highly conserved TCAT motif (residues 326–329 in Figure 2B). Changes in the P-loop are also much more dynamic than we had originally predicted (Supplemental Figure 6). Interactions with the residues 147–150 of the  $\alpha D$ - $\alpha E$  loop in the basal state are not recovered in the active state. Likewise Switch II and III, and  $\beta 4$  interact with variable degrees of binding intensity (as defined by ROSETTA Energy Units) with the P-loop suggesting more dynamic structural rearrangements in this region.

### 3.2.3. Receptor-induced network changes

As expected, the receptor-bound heterotrimer possesses an altered interaction network indicative of altered structure. These conformational changes are highlighted in interaction shifts along the  $\alpha 1$  helix and the  $\alpha 5$  helix (Figures 6–7) as these secondary structure elements move to make transient connections. Connections are also lost between Switch I and the Switch II/ $\beta 3$  interface during receptor binding, which are recovered upon  $G\alpha$  activation and dissociation.

On the backside of the  $G\alpha$  subunit, the P-loop, which has also been implicated in nucleotide stability and possible mechanisms of release [9,24,25] shows a drastic structural rearrangement and transition during receptor binding (Supplemental Figure 6). As observed above, the P-loop possesses a structural alteration resulting in a loss of interaction with the  $\alpha D$ - $\alpha E$  loop that is not present during receptor binding nor is it recovered post-dissociation in the monomeric, active state.

The linker 1 region connecting the helical domain to the GTPase domain via the  $\alpha 1$  to  $\alpha A$  helices also possesses a shift in conformation (Figure 6, Supplemental Figure 7). This element was hypothesized to be an important mechanistic feature to allow domain opening for nucleotide escape [10,24]. However some movement is expected as it does not possess any secondary structure elements.

### 3.2.4. The Helical Domain as a rigid body

Interesting secondary structural elements within the helical domain, such as the  $\alpha A$  helix, do not drastically alter their interaction networks across the three signaling states. This suggests that these elements move together while maintaining a similar tertiary fold (Supplemental Table 8, Supplemental Figure 8). These results are in agreement with DEER, EPR, NMR and crystallographic data [5,10,25], which suggests the helical domain moves as rigid body away from the nucleotide binding pocket [5,10,21].

## 4. Discussion and Conclusions

The heterotrimeric G protein undergoes dynamic changes in its structure and its binding affinity throughout the stages of the signaling cycle. We utilized structural models of these conformational states to analyze the energetic contributions that stabilize intra- and inter-molecular interactions that define these states, specifically within the  $G\alpha_{i1}$  subunit. This new analysis application predicts key amino acids to be nodes within the information network that propagate the signal across the complex upon interaction with the receptor.

Utilizing the ROSETTA software suite, we computed energy values for residue interactions along different binding interfaces. This benchmarked computational technique has been shown to provide useful insight in the following studies [16,17,26]. Likewise, ROSETTA was used to compute pairwise interactions between individual amino acids within the  $G\alpha$  subunit of the heterotrimeric G protein. This technique allowed us to compare the predicted thermodynamically stabilizing interactions between the basal, receptor-bound and activated conformations of the  $G\alpha$  subunit. Through this analysis we were able to detect intra-protein differences in amino acid interaction networks important for propagating conformational changes.

In a previous analysis [9] the  $G\alpha_{i1}$  subunit was evaluated in the basal, GDP-bound trimeric state and in the receptor-bound state through the use of  $\Delta\Delta G$  analysis. Our current study expands on this progress by also including the activated monomeric state for comparison of energy contributions made by key secondary structure elements to evaluate critical regions for G protein activation. In addition we have modeled all three signaling states to evaluate changes in residue pair contributions during signaling.

### 4.1. GDP- vs GTP-bound models

From this analysis, we have highlighted the similarity of the  $G\alpha_{i1}$  GDP- versus GTP-bound structures. By excising specific structural elements, a broad map of protein stability can be painted. Regions important for interfacing with other proteins, such as the  $\alpha 5$  helix and the Switch II domain show the most altered energy changes between these two states (Figure 4, Supplemental Table 2, 6). This is expected as the binding partners contribute to the relative energy of the system and inhibit interface flexibility. Regions not involved in protein-protein interactions or large structural rearrangements, such as the  $\alpha A$  helix (Supplemental Table 8), remain more energetically stable and consistent across the different models in the GDP and GTP-bound  $G\alpha$  subunit. This result is in agreement with other structural studies that suggest the helical domain moves as a rigid body throughout G protein activation [4,10,21,27].



#### 4.2. Receptor-induced activation

The  $\Delta\Delta G$  calculations serve to highlight the role of key secondary structure elements as well as specific non-structured linker regions in G protein activation via receptor coupling,  $R^* \cdot G_{\alpha_1}(\text{empty})\beta\gamma$ . During this structural transition state in which  $G\alpha$  must undergo a dynamic conformational change, the  $\Delta\Delta G$  analysis shows a shift in interaction partners for the  $\alpha 1$  helix,  $\alpha 5$  helix, and P-loop (Figures 3–4, Supplemental Tables 1–2, 4). This conformation must therefore propagate from the receptor to the helical domain of the  $G\alpha$  subunit in order to disrupt binding of GDP. Each of these elements has been implicated in the mechanism of nucleotide escape and G protein activation [22,24,25,28]. From this analysis alone, however, no direct conclusions could be made on the order or dynamics of conformational propagation across the subunit.

#### 4.3. Residue-Residue changes within the network

To better address this, a more detailed analysis of the structural differences was performed. The informational network mapping through the per-residue pairwise analysis highlighted subtle changes in G protein side chains induced by the  $\gamma$  phosphate group of the nucleotide. These altered interaction scores are indicative of altered structures which may prove to be important for interaction with downstream signaling and regulator moieties. However, we do not predict that all changes seen between these two states contribute to effector selectivity and interaction, as some of the altered network must be involved in maintaining the stability of the new structure without contributing to function.

Our pairwise analysis provides insight into possible routes of this information flow from the receptor to the nucleotide binding pocket. Through examination of the  $\alpha 1$  helix, the  $\alpha 5$  helix, and the P-loop, extreme displacement of the interaction pairs predicts the importance of these structural elements in allowing nucleotide exchange and G protein activation (Figures 6–7, Supplemental Figure 6). To further test and validate these predictions, additional experiments must be performed to further elucidate the mechanism of G protein activation.

From these analyses, we have created full, downloadable interaction matrices of our results to provide further understanding of G protein structure and modulation (Supplemental Material). By including pairwise score information across several signaling states, we hope this data will prompt new and unique questions on G protein activation and its signaling mechanics through investigation of these interactive communication maps. The values represent averaged relative interaction scores within these protein complexes as derived from comparative modeling based on published crystal structures. Future studies will be required to investigate the true predictive power of these results *in vitro*.

#### 4.4. Method development

The use of  $\Delta\Delta G$  calculations in evaluating protein-protein interfaces has long been an important application within ROSETTA [9,16,17,26]. We utilized this analysis not only for evaluating changes along known protein-protein interfaces, but also along key secondary structure elements thought to be important for propagating conformational changes across the protein subunit or necessary for stability. By mapping the  $\Delta\Delta G$  of critical structures across multiple models, we were able to compare

relative energy contributions as described by the ROSETTA score function for multiple structural snapshots.

One of the primary purposes for the creation of these energy calculations was to apply and validate a new method of interaction analysis available in the ROSETTA modeling software suite. Here we introduce a new methodology for evaluating the communication networks underlying three dimensional protein topology. By evaluating the residue-residue contributions to protein structure, we have created a technique to map interaction partners necessary for structural stability and conformation transmission. The ROSETTA score term for each contributing residue pair provides a roadmap for amino acid interactions necessary for both structure and function. This pairwise analysis also highlights key nodes of information flow when calculated across multiple protein structural states. The protocol utilized herein has been externally validated and made available for academic and public use with the ROSETTA software suite.

## 5. Downloadable Communication Maps

From these analyses, we have created downloadable interaction matrices available as supplementary material. They combine secondary structure stability with individual ROSETTA scores of interactions on a residue-residue level. This novel perspective has allowed us to begin to probe regionally specific interactions required for GPCR-G protein interaction, residues required to propagate intra-domain conformational changes, and stabilize the basal, receptor-bound, and activated  $G\alpha$  states. The download also possesses general features about the regional selection such as secondary structure elements, relative evolutionary conservation, amino acid composition etc. as specific to the  $G\alpha_{i1}$  subunit sequence.

## Acknowledgements

The authors would like to thank Dr. Rocco Moretti for creating the `residue_energy_breakdown` application within ROSETTA as well as Dr. Ali Kaya for reviewing the manuscript and for helpful discussion.

Funding for this work was provided by the NIH (R01 EY006062, R01 GM080403, R01 GM099842, R01 DK097376, R01 HL122010, R01 GM073151, U19 AI117905) and NSF (CHE 1305874).

## Conflicts of Interests

All authors declare no conflicts of interest in this manuscript.

## Author Contributions

AL performed the analyses, wrote the manuscript, created models for the signaling states, and wrote some of the scripts needed for analysis. JLK edited the manuscript, wrote some of the scripts needed for analysis, and validated the Protocol Capture. KK wrote some of the scripts needed for analysis. NA created models for the signaling states and wrote some of the scripts needed for

analysis. HH edited the manuscript and provided insight and discussion. JM planned the research, edited the manuscript, and provided guidance in protocol development.

## References

1. Hamm HE (1998) The Many Faces of G Protein Signaling. *J Biol Chem* 273: 669–672.
2. Sprang SR (1997) G proteins, effectors and GAPs: structure and mechanism. *Curr Opin Struct Biol* 7: 849–856.
3. Noel JP, Hamm HE, Sigler PB (1993) The 2.2 Å crystal structure of transducin- $\alpha$  complexed with GTP  $\gamma$  S. *Nature* 366: 654–663.
4. Van Eps N, Oldham WM, Hamm HE, et al. (2006) Structural and dynamical changes in an  $\alpha$ -subunit of a heterotrimeric G protein along the activation pathway. *Proc Natl Acad Sci U S A* 103: 16194–16199.
5. Rasmussen SG, DeVree BT, Zou Y, et al. (2011) Crystal structure of the beta2 adrenergic receptor-Gs protein complex. *Nature* 477: 549–555.
6. Cabrera-Vera TM, Vanhauwe J, Thomas TO, et al. (2003) Insights into G protein structure, function, and regulation. *Endocr Rev* 24: 765–781.
7. Oldham WM, Van Eps N, Preininger AM, et al. (2006) Mechanism of the receptor-catalyzed activation of heterotrimeric G proteins. *Nat Struct Mol Biol* 13: 772–777.
8. Yang CS, Skiba NP, Mazzoni MR, et al. (1999) Conformational changes at the carboxyl terminus of  $\alpha$  occur during G protein activation. *J Biol Chem* 274: 2379–2385.
9. Alexander NS, Preininger AM, Kaya AI, et al. (2014) Energetic analysis of the rhodopsin-G-protein complex links the  $\alpha 5$  helix to GDP release. *Nat Struct Mol Biol* 21: 56–63.
10. Van Eps N, Preininger AM, Alexander N, et al. (2011) Interaction of a G protein with an activated receptor opens the interdomain interface in the  $\alpha$  subunit. *Proc Natl Acad Sci U S A* 108: 9420–9424.
11. Ford CE, Skiba NP, Bae H, et al. (1998) Molecular basis for interactions of G protein  $\beta\gamma$  subunits with effectors. *Science* 280: 1271–1274.
12. Sondek J, Lambright DG, Noel JP, et al. (1994) GTPase mechanism of Gproteins from the 1.7-Å crystal structure of transducin  $\alpha$ -GDP-AIF-4. *Nature* 372: 276–279.
13. Sprang SR (1997) G protein mechanisms: insights from structural analysis. *Annu Rev Biochem* 66: 639–678.
14. Chivian D, Baker D (2006) Homology modeling using parametric alignment ensemble generation with consensus and energy-based model selection. *Nucleic Acids Res* 34: e112.
15. Raman S, Vernon R, Thompson J, et al. (2009) Structure prediction for CASP8 with all-atom refinement using Rosetta. *Proteins* 77 Suppl 9: 89–99.
16. Kortemme T, Baker D (2002) A simple physical model for binding energy hot spots in protein-protein complexes. *Proc Natl Acad Sci U S A* 99: 14116–14121.
17. Kellogg EH, Leaver-Fay A, Baker D (2011) Role of conformational sampling in computing mutation-induced changes in protein structure and stability. *Proteins* 79: 830–838.
18. DeLano WL (2002) Unraveling hot spots in binding interfaces: progress and challenges. *Curr Opin Struct Biol* 12: 14–20.
19. Lazaridis T, Karplus M (1999) Effective energy function for proteins in solution. *Proteins* 35: 133–152.

20. Lazaridis T, Karplus M (1999) Discrimination of the native from misfolded protein models with an energy function including implicit solvation. *J Mol Biol* 288: 477–487.
21. Westfield GH, Rasmussen SG, Su M, et al. (2011) Structural flexibility of the G alpha s alpha-helical domain in the beta2-adrenoceptor Gs complex. *Proc Natl Acad Sci U S A* 108: 16086–16091.
22. Coleman DE, Berghuis AM, Lee E, et al. (1994) Structures of active conformations of Gi alpha 1 and the mechanism of GTP hydrolysis. *Science* 265: 1405–1412.
23. Mixon MB, Lee E, Coleman DE, et al. (1995) Tertiary and quaternary structural changes in Gi alpha 1 induced by GTP hydrolysis. *Science* 270: 954–960.
24. Kaya AI, Lokits AD, Gilbert JA, et al. (2014) A conserved phenylalanine as relay between the  $\alpha 5$  helix and the GDP binding region of heterotrimeric Gi protein  $\alpha$  subunit. *J Biol Chem*.
25. Ceruso MA, Periole X, Weinstein H (2004) Molecular dynamics simulations of transducin: interdomain and front to back communication in activation and nucleotide exchange. *J Mol Biol* 338: 469–481.
26. Sharabi O, Shirian J, Shifman JM (2013) Predicting affinity- and specificity-enhancing mutations at protein-protein interfaces. *Biochem Soc Trans* 41: 1166–1169.
27. Oldham WM, Van Eps N, Preininger AM, et al. (2007) Mapping allosteric connections from the receptor to the nucleotide-binding pocket of heterotrimeric G proteins. *Proc Natl Acad Sci U S A* 104: 7927–7932.
28. Kapoor N, Menon ST, Chauhan R, et al. (2009) Structural evidence for a sequential release mechanism for activation of heterotrimeric G proteins. *J Mol Biol* 393: 882–897.



AIMS Press

© 2015 Jens Meiler, et al., licensee AIMS Press. This is an open access article distributed under the terms of the Creative Commons Attribution License (<http://creativecommons.org/licenses/by/4.0>)